

High Surface Area Titania Photocatalytic Microfluidic Reactors

Henrik Lindstrom

Intl. Centre for Young Scientists (ICYS), Natl. Institute for Materials Science (NIMS), 1-1 Namiki, Tsukuba, Ibaraki 305-0044, Japan

Robert Wootton

John Moores University, Dept. of Pharmacy and Chemistry, Byrom Street, Liverpool L3 3AF, U.K.

Alexander Iles

Intl. Centre for Young Scientists (ICYS), Natl. Institute for Materials Science (NIMS), 1-1 Namiki, Tsukuba, Ibaraki 305-0044, Japan; and Univ. of Hull, Dept. of Chemistry, Cottingham Road, Hull HU6 7RX, U.K.

DOI 10.1002/aic.11096

Published online February 2, 2007 in Wiley InterScience (www.interscience.wiley.com).

In this work a simple method is described for depositing a robust yet highly porous film of anatase titania nanoparticles with a very high surface area onto the inside walls of microfluidic devices. A very high loading of 66 g of titania per liter of reactant solution was achieved. The effectiveness is demonstrated of this deposition method by producing functionalized microfluidic reactor devices and using them to photocatalytically degrade air-saturated methylene blue solutions. Experiments were performed with and without the addition of gaseous oxygen to the microreactors. The addition of oxygen dramatically enhanced the degradation rate. This highlights the necessity for supplying additional oxygen to microsystems during photocatalysis since dissolved oxygen can be rapidly depleted within the small confined space inside microreactors. With additional gaseous oxygen, the conversion rate for the photodegradation reaction of 0.1mM methylene blue at a flow rate of 12 $\mu\text{L min}^{-1}$ was 10.6 % s^{-1} . © 2007 American Institute of Chemical Engineers AICHE J, 53: 695–702, 2007

Keywords: titanium dioxide, anatase, photocatalysis, microreactor fabrication

Introduction

Titanium dioxide has enormous potential for use in applications such as photocatalytic synthesis and the photodegradation of persistent organic compounds.^{1,2} However, despite extensive research, the widespread use of titanium dioxide in such applications has been restricted due to difficulties in constructing a practical system incorporating this photocatalyst. Typical macroscale systems have involved the suspension of

a titanium dioxide powder in an aqueous solution, which is then exposed to UV light. Efficient light coupling and the subsequent removal of the catalyst from the solution can be problematic.^{3,4} Immobilized systems can be used to overcome the problem of post process separation, although they tend to have smaller interfacial surface areas and can be difficult to apply at larger scales.^{5,6}

Microfluidic devices have the potential to be highly effective for use as photocatalytic reactors due to their inherently large surface area to volume ratio and ease of interfacing with UV light. Although the output of a single device is small, throughput can be increased by connecting many devices in parallel.⁷ A number of researchers have investigated

Correspondence concerning this article should be addressed to A. Iles at a.iles@hull.ac.uk.

the possibility of using immobilized titanium dioxide in photocatalytic microsystems.

The group of Maeda investigated the deposition of titanium dioxide in capillaries.^{8,9} This was based on the production of a film of silica/titania nanocomposites, held together with an organic surfactant. The performance of this system was compared to a monolayer of titania nanoparticles in a capillary and also to a batch process. Both capillary systems were capable of decolorizing an aqueous methylene blue (MB) solution and were more effective than the comparable batch process. However, the monolayer system had a small active surface area and, although the surface area of the nanocomposite was larger, it is questionable as to whether these organic/inorganic structures would be robust enough to survive extended periods in the harsh environment found inside such a microreactor.

Gorges et al. used anodic spark deposition to create a film of titania on a microstructured ceramic substrate that was then bonded to a glass top plate.¹⁰ A UV-LED array was utilized so that a fully solid state system could be realized for the photodegradation of 4-chlorophenol. The nature of this fabrication method meant that the film porosity was variable and only 30% of it was of the photoactive anatase form. Also, since the substrate material was not transparent, it would not have been possible to stack multiple devices and maximize UV light usage.

The group of Kitamori investigated the use of sol-gel methods to deposit a porous titania film for use inside a microreactor.¹¹ The film produced covered only one surface inside the channel. XRD measurements showed that anatase titania was present, but the proportion of anatase to rutile in the film was not reported. The surface area of the film was relatively low since it was only 300 nm thick and was composed of 100 nm size particles. The device was used to perform a redox-combined synthesis, but the productivity of the system was poor due to surface area limitations. MB photodegradation was also performed, although no data were provided.

Recently, Jones et al. fabricated several types of photocatalytic microreactors for protein cleavage.¹² These were based on the use of titania coated glass, or titania sol gel coated silica particles. The available surface area and the proportion of anatase to rutile titania were not discussed.

A practical microfluidic photocatalytic reactor must have a very large active surface area, be simple and cheap to produce, yet be robust enough to be used for long periods without maintenance. Previously reported systems have not met all of these rigorous requirements. Nanoporous TiO₂ films have been studied intensively for their use as electrodes in applications such as solar cells, rechargeable batteries, electrochemical synthesis and for smart window/display systems.¹³ These μm deep films typically consist of a highly permeable network of interconnected nanometer sized particles. Reactant solution enters the pore channels and establishes contact with each particle; hence, heterogeneous redox reactions can occur at the inner surface throughout the entire volume of the film. The idea behind this study was to combine the beneficial properties of these nanoporous films with microfluidic devices to produce highly effective systems for photocatalysis. Hence, in this work we describe a simple technique for depositing a robust, nanoporous large surface area TiO₂ film onto the inside walls of microfluidic reactor devices.

Methylene blue (MB) has been used as a model compound to demonstrate the performance of numerous bulk scale titania based photodegradation systems. These studies have shown that the efficiency of the degradation process is dependent upon a number of factors, including: photocatalyst particle size and loading, temperature, light intensity, solution pH, and the dissolved oxygen concentration (DOC).^{14–16} It is generally assumed that degradation occurs predominantly via the formation of powerful oxidizing species such as hydroxyl radicals on the surface of the photocatalyst during illumination. However, the efficiency of hydroxyl radical formation is strongly dependent on the DOC, since the presence of oxygen suppresses electron/hole recombination by scavenging electrons. It has been shown that when the DOC is below 5 mg l⁻¹, the degradation rate of MB by TiO₂ is severely affected.¹⁶ Furthermore, if the DOC drops below 0.32 mg l⁻¹, then the reduced, colorless form of MB, leucomethylene blue (LMB), is rapidly formed. This is a reversible photo-bleaching effect, not a degradation reaction, which indicates that the hydroxyl radical formation process is extremely inefficient in the absence of dissolved oxygen. The exposure of LMB solutions to oxygen reverses the decolorization process. Hence, as noted by Mills et al.,¹⁷ when using the change in red light absorbance of MB solutions to measure the extent of photodegradation, it is critically important to expose the reacted solutions to air, before performing measurements.

The effectiveness of the devices produced using our new technique was demonstrated by applying them to the photodegradation of MB. None of the previously reported microscale systems were operated with additional oxygen. The solubility of oxygen in water is relatively low and, in a microfluidic photodegradation system, the dissolved oxygen is likely to be depleted very quickly, especially if the photodegradation rate is high. However, a major advantage of microfluidic systems is that gasses such as oxygen and solutions can be efficiently manipulated and mixed within a single device. We show that the effectiveness of microfluidic catalytic photodegradation reactors can be significantly enhanced by supplying additional oxygen to these systems. Although in many respects, microfluidic reactors are potentially an ideal platform for photodegradation reactions, we suggest that such systems are ultimately limited by the availability of oxygen inside the microchannels of a device.

Experimental

Microfluidic device fabrication

1.5 mm thick soda-lime glass blank wafers, as well as wafers pre-coated with low reflective chromium and photoresist, were obtained from Nanofilm (Westlake, USA). The coated wafers were micro-patterned using direct write laser lithography (DWL, Heidelberg Instruments, Germany); and a serpentine channel with two inlets and one outlet, as shown in Figure 1, was wet-etched into the glass to the desired depth (50 μm) using buffered NH₄F/HF solution. The inner area and volume of the etched chip were calculated to be 1.58 cm² and 2.97 μl , respectively. The projected area was measured to be 0.53 cm². After etching, access holes were drilled ultrasonically (SOM-21, Shinoda, Tokyo, Japan). Prior to bonding, the wafer surfaces were degreased with acetone

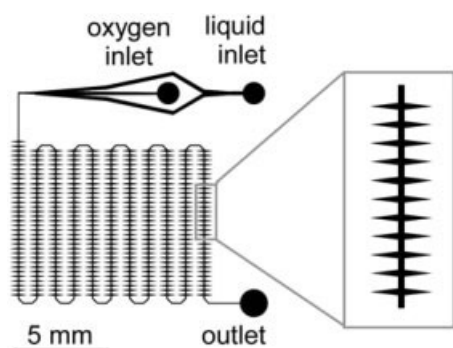


Figure 1. Chip design.

The microfluidic reactor contained 11 rows with 32 side lobes per row to increase surface area. It was isotropically etched to a depth of 50 μm , and the channel width was approximately 150 μm . Note the secondary inlet for oxygen introduction (if required).

and then iso-propanol. Subsequently, the surfaces were immersed in heated piranha solution for 1 h. The wafers were then washed with deionized water and were ready for bonding. The structured wafer was then thermally bonded to a blank sealing wafer by applying slight pressure and heating to 570°C for 10 h in air. After bonding, silica capillaries (150 μm i.d., Polymicro, USA) were glued into the access holes using Araldite 2014 (RS Components, Corby, UK).

Deposition method

A colloidal TiO_2 suspension of a suitable loading was manufactured using Ishihara STS-01 (Ishihara Sangyo, Osaka, Japan). The best deposition results were obtained when a colloid of 11% dry content was used. The appropriate concentration was obtained by diluting the STS-01 suspension with nitric acid of pH 1. The suspension was sonicated for 30 min before usage to ensure homogenous dispersion. Before filling the microdevices with TiO_2 suspension, the channels were flushed with a solution of 2 M NaOH for 20 min and were subsequently flushed with deionized water. The microdevices were filled with TiO_2 suspension using a syringe pump (Harvard Apparatus 11 Plus). Then, nitrogen gas was pumped through these devices to remove the excess TiO_2 suspension. The TiO_2 treated chips were then heated in air at 400°C for 6 h.

Film analysis and methylene blue degradation

Microstructural observations of TiO_2 layers deposited onto the channel walls in the microfluidic chips were performed using an optical microscope (Nikon Eclipse TE 2000-U) and a field emission scanning electron microscope (Hitachi S-4800). Well-defined cross sections of the coated channels were obtained by scribing the bonded chips on the upper and lower sides with a diamond cutter and subsequently breaking the chip apart along the scribe lines.

The surface area of the TiO_2 layer was obtained by BET measurements (Quantachrome Autosorb-1 sorption analyzer). The samples were outgassed at 200°C for 1 h before the adsorption measurements. The specific surface area calculation was based on a seven-point measurement. The powder used for the surface area and XRD analyses was prepared by

depositing a one micron thick layer of TiO_2 suspension onto a large glass plate and heating the deposited layer in air at 400°C for 6 h. The heated layer was then scraped off the glass plate yielding millimeter and submillimeter flakes of sintered particles. The specific surface area was calculated using the BET method. The crystal structure of the powders was determined by X-ray diffraction (RINT 2200, Rigaku) using $\text{CuK}\alpha$ radiation. The porosity of the deposited film was obtained by a method described previously.¹⁸

Photocatalytic reactions were carried out by illuminating the microreactors with UV-light from a combined mercury-xenon arc lamp (Supercure-352S, San-Ei Electric). This lamp was equipped with a light guide. For each experiment, a microreactor was placed 2.5 cm from the UV lamp light-guide while a 0.1 mM solution of methylene blue (MB) (Fluka; +97%) in deionized water of pH 7.0 was pumped through the device using a syringe pump. According to literature, this concentration can be estimated to result in a mixture of 59% dimeric- and 41% monomeric MB.¹⁷ The photodegraded solution was collected in a closed plastic vial in order to prevent the evaporation of solvent during the course of the experiment. Gaseous oxygen was introduced into the microreactors as required, by connecting an oxygen cylinder via a reduction regulator. This produced alternating plugs of liquid and gas traveling through the microfluidic channel. The pressure of the gas was adjusted so that the plugs of gas and liquid in the channel were of a similar length (approximately 4mm). Hence, this reduced the liquid residence time by approximately a factor of two. The reactant solutions were analyzed using absorption spectroscopy. Absorbance spectra were obtained using quartz cuvettes and a UV-VIS-NIR spectrophotometer (Jasco V-570).

Lamp spectral intensity measurements were performed with a Spectroradiometer (Ushio USR-30) positioned at the working distance (2.5 cm from the end of the light guide). The total integrated incident intensity between 200 and 800 nm from the UV lamp was 1.0 W cm^{-2} . A layer of glass of the type used for the chip substrate material was placed between the light guide and the spectroradiometer so that the total integrated intensity spectrum impinging on the TiO_2 layer inside the chip device could be estimated. This was found to be 625 mW cm^{-2} , which means that 375 mW cm^{-2} was lost due to reflection losses and absorption in the glass. A similar measurement was then performed with a 2 μm thick TiO_2 film deposited onto a layer of substrate glass. The total transmitted integrated intensity of this spectrum was 474 mW cm^{-2} , which means that 526 mW cm^{-2} was lost due to reflection losses and absorption in the glass and TiO_2 . Adding these losses gives 900 mW cm^{-2} and, hence, approximately 100 mW cm^{-2} is absorbed in the TiO_2 layer. The amount of light that was absorbed in the chip was also calculated from spectral intensity measurements on the chip glass substrate (see above) and absorption measurements of a 2 μm thick film of titania particles on a quartz sheet using an integrating sphere (Jasco V-570). This calculated integrated absorbed power within the TiO_2 layer was 111 mW cm^{-2} , that is, close to 100 mW cm^{-2} , verifying that the absorption measurement was reasonably correct. No correction for reflection was made for the TiO_2 coated quartz slide and, hence, a value of 111 mW cm^{-2} is the upper limit of light absorption in the TiO_2 layer. The geometry of the chip made it difficult to estimate the magnitude of the error intro-

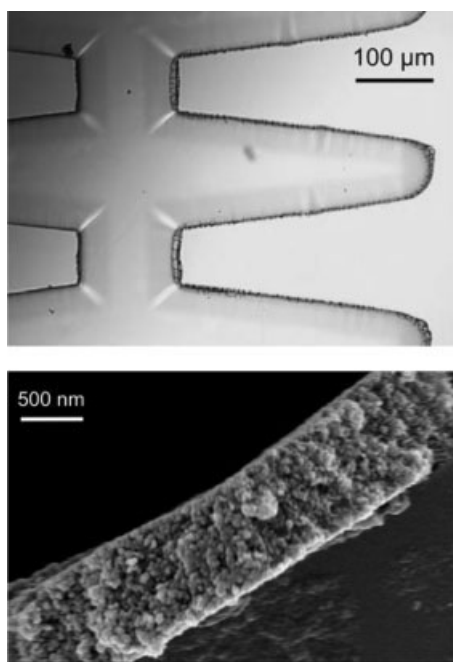


Figure 2. (Top) Microscope top view picture of a micro-reactor with a TiO₂ film deposited onto the walls (magnification ×200); (bottom) Cross sectional SEM picture of deposited TiO₂ layer onto the walls inside a microreactor.

duced for the approximation used for the effective film thickness. This is because optical effects such as light scattering and light reflection might increase or decrease light absorption in the TiO₂ layer.

The stability of the lamp system was monitored over a period of 3.5 days using a photodiode. The maximum variation in the light intensity from the lamp during this period was $\pm 8\%$.

To estimate the amount of MB adsorbed onto the surface of the TiO₂ inside the microdevice, we mixed 0.066 g of sintered TiO₂ powder (obtained from STS-01 suspension) with 1 g of MB solution at 0.1 mM MB in a vial and measured the absorbance change of the MB solution after equilibration. The ratio of 66 g of TiO₂ to 1 liter of MB solution corresponded to the estimated ratio between the amount of MB solution and TiO₂ in the microfluidic chip.

Results and Discussion

As can be seen from optical and SEM observations (Figure 2), a porous film of titania was deposited on the inside of the microreactors using the method described, even though the geometry of the chip layout was relatively complex. The film thickness was roughly 1 μm. The porosity of the TiO₂ layer was measured to be 67%. An 11% titania solution was found to give the best results. Higher concentrations produced films that cracked and peeled after drying. By taking the inner surface area of the etched channel walls (1.57 cm²), the film porosity, the density of anatase, and the layer thickness, we estimated the total photoactive TiO₂ surface area inside the chip to be roughly 520 cm². The film proved to be very robust, in terms of its mechanical stability;

it did not crack or peel even after several days of continuous operation. However, the film could be removed by pumping alkaline solutions through the device, such as 2.0 M sodium hydroxide. This delamination was probably due to the sodium hydroxide attacking the glass channel walls.

Figure 3 shows X-ray diffraction patterns of the TiO₂ films that were heated to different temperatures for 6 h. All diffraction peaks in all spectra can be attributed to the anatase polymorph, the most photoactive form of titania. The estimated particle size using the Scherrer equation¹⁹ was roughly 7 nm, 12 nm, and 15 nm for temperatures of 70°C, 400°C, and 450°C, respectively. Hence, heating to 400–450°C led to a certain amount of particle growth. In this work we used a sintering temperature of 400°C, which means that assuming a mean particle diameter of 12 nm, a 1 μm thick film would have a depth of about 83 particles. The high porosity in combination with the small particle size resulted in a surface area of this deposited film of 260 m² g⁻¹, which is about seven times higher than previously reported values for films of titania deposited within photocatalytic microreactors.¹⁰ Films heated at low temperatures were not sufficiently robust. Films heated to 450°C resulted in an anatase film with a smaller BET surface area (130 m² g⁻¹). Consequently, for our devices we heated the films to 400°C to consolidate the film, produce a robust layer, and achieve as large a surface area in the channels as possible.

The results of the application of our photocatalytic microreactors to the degradation of methylene blue are shown in Figure 4. The decrease in the peak intensity at 664 nm was used as a measure of the amount of degradation. A 9% decrease in absorbance, corresponding to a degradation rate of 0.30 % s⁻¹ (effective residence time 30 s), was observed under UV illumination when MB solution and oxygen were pumped through a chip without a TiO₂ film. The degradation of MB by UV alone is a well-known effect.²⁰ The reactant solutions did not change color once exposed to air, which indicates that the intensity decrease was due to degradation and not due to formation of the reduced MB form.

The presence of the titania film had a significant effect on the concentration of MB observed in the effluent. A 38%

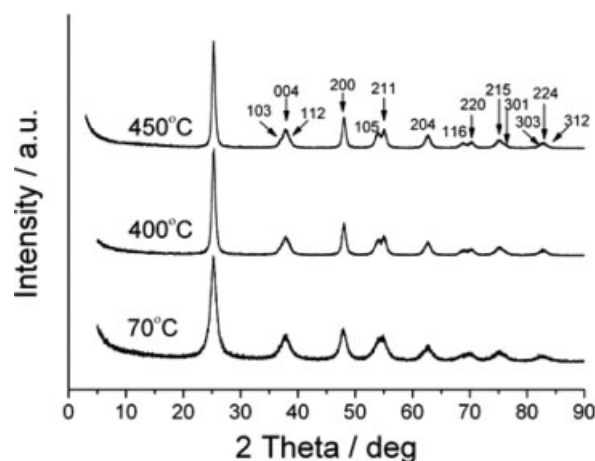


Figure 3. XRD patterns for deposited TiO₂ films heated to different temperatures for 6 h.

Crystallographic planes are indicated for each peak.

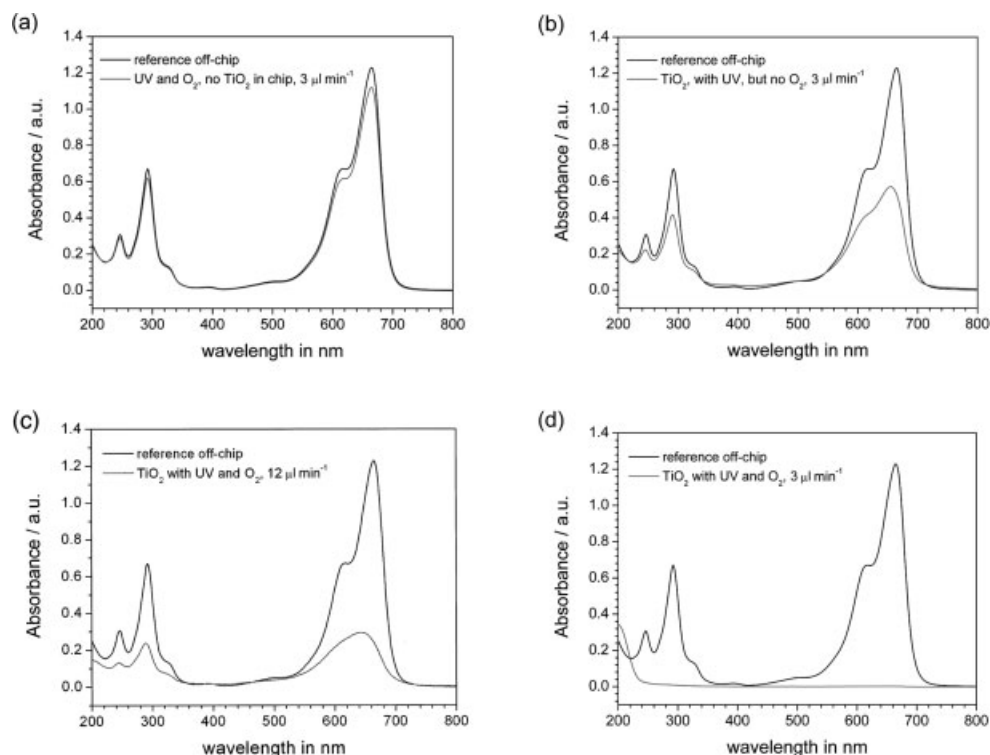


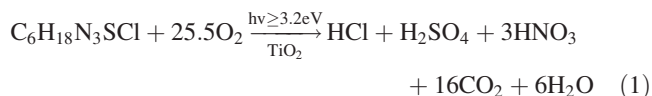
Figure 4. Absorbance spectra of four chip effluents and one reference solution; the methylene blue absorption peaks decreased according to the extent of degradation.

All experiments were performed over a period of more than 24 h. (a) The reference solution (0.1 mM MB) compared with a 0.1 mM MB solution pumped at $3 \mu\text{l min}^{-1}$ through a UV exposed chip without a TiO_2 coating and with oxygen. (b) The reference solution compared with a 0.1 mM MB solution pumped at $3 \mu\text{l min}^{-1}$ through a UV exposed chip with a TiO_2 coating and without oxygen. (c) and (d) The reference solution compared with a 0.1 mM MB solution pumped at 12 and $3 \mu\text{l min}^{-1}$, respectively, through a UV exposed chip with a TiO_2 coating and with oxygen.

decrease in absorbance was observed when an aerated MB solution was pumped through a TiO_2 coated chip at $3 \mu\text{l min}^{-1}$ and exposed to UV light; see Figure 4. This corresponds to a conversion rate of $0.63 \% \text{ s}^{-1}$ (residence time 60 s). The addition of oxygen to the TiO_2 coated microdevices had a dramatic effect on the degradation process. Even though the introduction of gaseous oxygen reduced the residence time of the solution within the microdevice, a 99.9% decrease in absorbance was observed when pumping MB solution at $3 \mu\text{l min}^{-1}$ and oxygen gas through the UV exposed TiO_2 coated chip. This corresponds to a conversion rate of $3.33 \% \text{ s}^{-1}$ (effective residence time 30 s). It can be seen that between 300 and 800 nm, the absorbance has been reduced almost to zero. Below 250 nm, an increase in absorbance can be observed. This is probably due to the oxidation of the nitrogen and sulfur in the methylene blue to produce nitrates and sulphates; see Eq. 1 below.²¹ Figure 4 also shows the spectrum obtained from MB solution pumped at $12 \mu\text{l min}^{-1}$ through the UV exposed TiO_2 coated chip in the presence of additional gaseous oxygen. As can be seen, an 80% decrease (effective residence time 7.5 s, conversion rate: $10.6 \% \text{ s}^{-1}$) was still observed, even at this higher flow rate.

Our MB reactant solutions did not regain their color after exposure to air, which strongly indicates that the LMB form of MB was not produced and that truly irreversible photodegradation of MB was achieved. The enormous difference

between the photodegradation of an aerated solution and a solution with additional gaseous oxygen can be attributed to the difference in the amount of available oxygen in the microchannels in these two experiments. The reaction for the complete degradation of MB is shown below:



As can be seen from Eq. 1 above, a 0.1 mM solution of MB, as used in these experiments, would require 2.55 mM of oxygen for complete degradation. However, an air-saturated solution at room temperature and atmospheric pressure can only contain 0.25 mM of dissolved oxygen. In the minute confined space within our microfluidic devices, we have a high light intensity, a high concentration of MB, and a large active TiO_2 surface area. Hence, the dissolved oxygen in the aerated MB solutions can be depleted rapidly by photoreactions. Pumping both oxygen and MB solution through the chip ensures the availability of oxygen throughout the microfluidic network at any given time. This observation highlights the importance of providing a sufficient amount of oxygen when performing photodegradation processes within microfluidic chips. There are many reasons why oxygen improves the photodegradation rate of methylene blue:

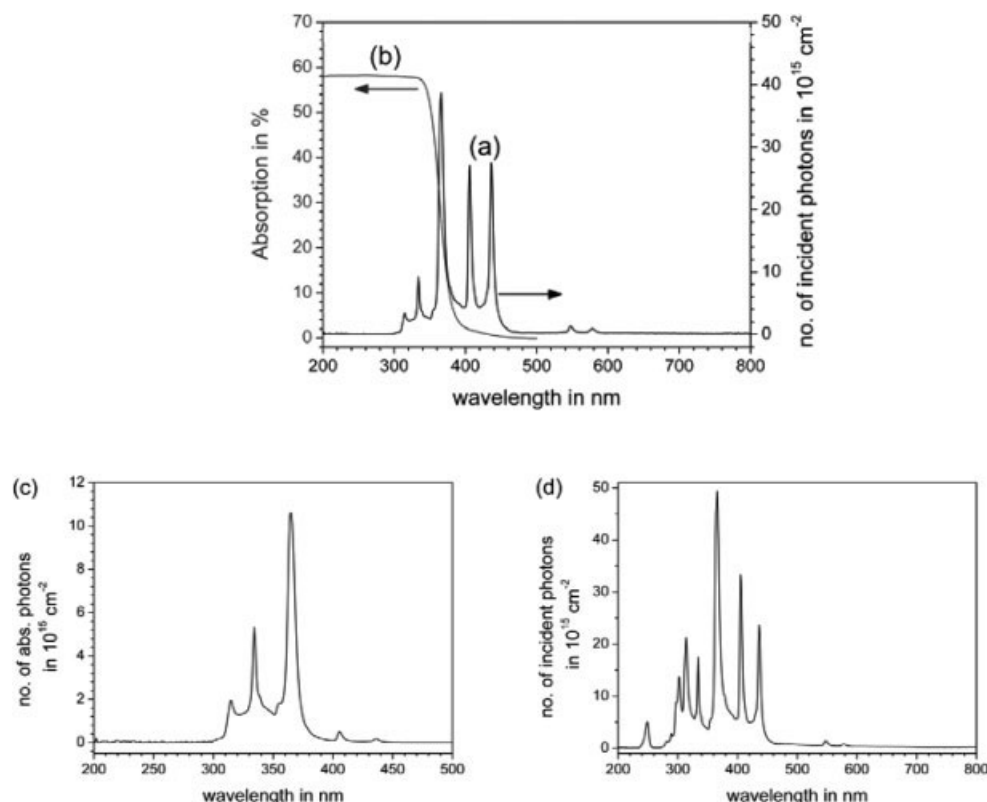


Figure 5. (a) Spectral intensity distribution measured for light that has passed through a single, bare glass chip substrate; (b) absorption spectrum of a 2.0 μm thick anatase film deposited on a quartz slide. (c) Calculated intensity distribution of absorbed photons in the TiO_2 film. (d) Spectral output of the lamp.

(a) Oxygen suppresses direct electron-hole recombination within the particles by acting as an electron acceptor at the TiO_2 surface forming O_2^- , which is a powerful oxidant. The removal of electrons also improves the charge separation and creates more holes and OH radicals that are then available for photodegradation of MB.

(b) The oxygen prevents MB from being reduced into the leuco form LMB at the TiO_2 surface by competing kinetically with MB in electron acceptance at the TiO_2 surface.

(c) Oxygen rapidly oxidizes any LMB that is formed back into the MB form and, in the process, produces O^{2-} .

(d) Pumping oxygen through the chip effectively improves the mass transfer by increasing the mixing of reactants in the reactor.

In an attempt to determine the number of photons absorbed in the deposited TiO_2 layer inside the chip, we approximated the effective light absorbing path length of TiO_2 inside the channels to be 2 μm , since SEM pictures revealed that the TiO_2 films were roughly 1 μm thick on each surface. The spectral intensity distribution of the light reaching the TiO_2 on the channel walls in our microdevices is plotted in Figure 5a. The absorption spectrum of a 2.0 μm thick TiO_2 film deposited on quartz is also plotted in Figure 5b. As can be seen, the TiO_2 film only absorbs a small fraction of the light that has passed through one bare glass chip substrate. Figure 5c shows the intensity distribution of the absorbed photons in the TiO_2 layer as obtained from Figures 5a and 5b. We calculated the total power absorbed in the deposited TiO_2 film

to be 59 mW and the total number of photons absorbed in the TiO_2 film to be $1.0 \times 10^{17} \text{ s}^{-1}$. This level of power means that our system was operated in a regime where the reaction rate was independent of light intensity.²² Flow rates of 3 $\mu\text{l min}^{-1}$ and 12 $\mu\text{l min}^{-1}$ correspond to 3.0×10^{12} and 1.2×10^{13} MB molecules passing through the chip per second, respectively. Hence, the number of photogenerated charge carriers was far in excess of the number of MB molecules. Although the total mineralization of one MB molecule requires 102 oxidizing equivalents that must be produced by photoelectrochemical reactions,¹⁷ there were still more than enough photons to perform the complete photodegradation of MB. However, even though there were sufficient photons available for the reaction, at a flow rate of 3 $\mu\text{l min}^{-1}$ MB was not completely destroyed unless additional oxygen was present. This shows that light intensity alone is not sufficient to achieve TiO_2 catalyzed MB photodegradation since without the presence of adequate oxygen, the formation of oxidizing species is extremely inefficient.

At the higher flow rate of 12 $\mu\text{l min}^{-1}$ with added oxygen, complete destruction was not achieved, despite the high photon flux. Hence, the influence of mass transfer effects on the photodegradation efficiency must be evaluated. Fast mass transfer of MB to the TiO_2 on the channel walls and fast mass transfer inside the TiO_2 film combined with strong adsorption of MB onto the surface of the TiO_2 are essential for efficient photochemical degradation. From the Einstein relation for molecular diffusion, we estimated the average

time for an MB molecule to reach the channel walls to be approximately 10 s (assuming an average traveling distance of 35 μm for MB molecules in this microfluidic geometry and an MB diffusion coefficient of $5.7 \times 10^{-6} \text{ cm}^2 \text{ s}^{-1}$).²³ Without the supply of additional oxygen, the flow rates of 12 and 3 $\mu\text{L min}^{-1}$ used in this article resulted in maximum residence times of 15 s and 60 s, respectively. Assuming perfect laminar flow and negligible MB adsorption onto the TiO_2 particles, then the average MB molecule would contact the TiO_2 layer only 1.5 or 6 times (at 12 $\mu\text{L min}^{-1}$ and 3 $\mu\text{L min}^{-1}$, respectively) during passage through the chip. However, experiments with sintered powder and MB solutions (see Experimental section) showed that the adsorption interaction between MB molecules and TiO_2 is fairly strong. Additionally, the average time for an MB molecule to diffuse through a 1 μm porous TiO_2 film can be estimated to be roughly 1 ms using an obstruction factor of two.²⁴ Therefore, the diffusion of MB through the porous TiO_2 layer is also not a limiting factor. These estimates indicate that there are no mass transfer limitations in this system and the degradation process is limited by intrinsic reaction kinetics.

Previously, Gorges et al. showed how mass transfer limitations in microfluidic reactors containing porous photocatalysts can be estimated from the Damköhler number, D_{aII} :¹⁰

$$D_{\text{aII}} = \frac{k_a \cdot d_h}{3.66 \cdot A \cdot D \cdot (K^{-1} + c_b)} \quad (2)$$

where k_a is the apparent system dependent rate constant, d_h the hydrodynamic diameter ($d_h = 6.6 \times 10^{-4} \text{ dm}$), A the interfacial area per unit volume of the TiO_2 film ($A = 3340 \text{ dm}^{-1}$), D the molecular diffusion coefficient, K the Langmuir adsorption coefficient, and c_b the bulk concentration of the solution ($c_b = 10^{-4} \text{ M}$). For D_{aII} values of less than 0.1, the reaction rate can be considered limited by the intrinsic kinetics of the photoreactions. Substituting parameters with values obtained from the literature ($k_a = 9.9 \times 10^{-8} \text{ M}^{-1} \text{ s}^{-1}$,²¹ $D_{\text{MB}} = 5.7 \times 10^{-8} \text{ dm}^2 \text{ s}^{-1}$,²³ and $K_{\text{MB}} = 20 \text{ mM}^{-1}$ ¹⁶) results in a maximal D_{aII} value of 6.3×10^{-4} when using the highest figure for k_a in the literature, which again verifies that the photoreaction rate is not limited by mass transfer of MB. Having excluded photon flux and MB mass transfer effects, the limiting factor for MB photodegradation in this system can only be attributed to the mass transfer of oxygen. In order to estimate the Damköhler number for oxygen, it is necessary to determine the bulk concentration of dissolved oxygen in the microchannel. However, it was not possible to estimate the rate and homogeneity of the dissolved gas distribution within the microchannel when additional oxygen was supplied, and so the D_{aII} value for this system could not be calculated.

Li et al.⁸ fabricated photocatalytic microreactors by depositing composite silica-titania anatase structures, held together with a surfactant, polyethyleneimine (PEI). In the harsh environment found inside a titania photoreactor, we were concerned as to whether PEI would remain unaffected. Hence, we obtained a sample of PEI (Wako Pure Chemical; average M_w 600), prepared a 40 mg l^{-1} solution of this surfactant and passed it through one of our photocatalytic microreactors, in both the presence and absence of added oxygen.

As can be seen from Figure 6, the absorption spectra of the PEI after passing through the device are significantly different, especially when additional oxygen is present. This

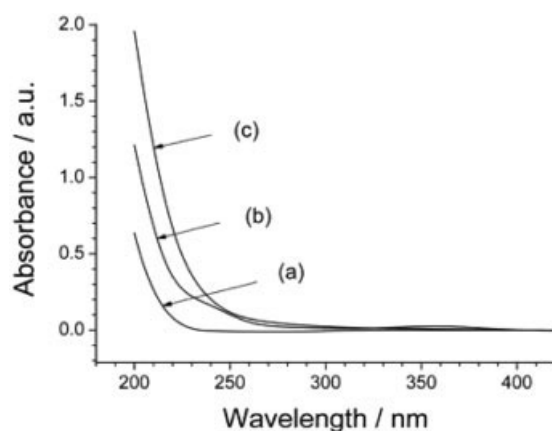


Figure 6. Absorbance spectra of polyethylene imine (PEI) solutions.

(a) Reference solution 40 mg l^{-1} . (b) PEI in aerated water (40 mg l^{-1}) photodegraded using a TiO_2 coated microreactor exposed to UV light. (c) PEI solution (40 mg l^{-1}) photodegraded using a TiO_2 coated microreactor exposed to UV light with the addition of gaseous oxygen. The flow rate in each case was 3 $\mu\text{L min}^{-1}$.

shows that PEI is seriously affected by contact with anatase titania and UV light. The increase in absorbance that can be observed in the far UV is probably due to the oxidation of the organic nitrogen within PEI to form nitrates.²⁵ Although Li et al. did not report on the long term stability of their system, our experiments show that it is unlikely that such composite structures would be suitable for long term operation within a photocatalytic microreactor.

In order to establish the robustness of our devices, we investigated the effects of running a microreactor continuously over a period of several days. A high flow rate (12 $\mu\text{L min}^{-1}$) of MB was used and additional oxygen was not supplied. This was to see whether the microreactor would be overwhelmed under such conditions. Effluent samples were collected at intervals from the device. Some variation was noted, although this was within what would be expected due to lamp output variations. Even after extended periods of operation, no deterioration in device performance was observed.

Previously reported photocatalytic microreactors fabricated using sol gel and spark deposition methods involved several complicated fabrication steps and produced devices where only one surface was coated. Our deposition process involves a simple modification to conventional chip fabrication methods. All surfaces inside the device are coated, and the method can be applied to a wide range of pre-manufactured microfluidic devices. For our experiments, we used soda lime glass as it is cheap, readily available, and easy to work with. It is also sufficiently UV transparent (89.5% transparent for a 1.5 mm thick substrate at 365 nm). The use of quartz substrates could be used to improve performance, as this would allow the effective use of deep UV lines from the lamp that would be more readily absorbed by the TiO_2 film.

The microreactors used in this work were not specifically designed for photocatalysis, and so there is significant room for design optimization. With a simple redesign, the chip layout could be improved to maximize the available surface area and improve gas/liquid mixing. The lamp system is not

particularly efficient, and it cannot be used for more than 1000 h before the lamp must be exchanged. This could be replaced with an LED system, which would mean that a robust, low power, low cost, fully solid state system could be realized. Such a system could be operated for very long periods of time without maintenance. Further improvements could be made by enhancing the light coupling to the system and by operating multiple devices in parallel. These devices could be illuminated from both sides to increase the absorbed light intensity or even stacked to maximize the efficient usage of available light.

Conclusions

We have shown that it is possible to deposit a highly porous anatase film with a very high surface area onto the inside walls of microreactor devices and have demonstrated that such devices can be used for photodegradation. These devices were found to be very robust and could operate for long periods of time without loss of performance. Photocatalytic devices fabricated using our new method could be used in an enormous range of different catalysis systems, not just for photodegradation. Hence, it is likely that they will be utilized in many different areas of chemistry and biochemistry.

Microreactors are potentially an ideal platform for photocatalysis since a large amount of light can be absorbed in a thin, immobilized, high surface area photoactive layer held within a very small volume that can be efficiently coupled to a light source. As we have shown, an extremely high loading factor of 66 g of anatase TiO₂ per liter of MB solution can be realized while maintaining homogenous excitation in the photoactive layer. Such a high loading with a macroscale suspension system would be extremely inefficient since homogeneous excitation would not be possible. Furthermore, although the small confined space within a microreactor limits the availability of oxygen, which plays a significant role in photodegradation processes, gaseous oxygen can be added to overcome this limitation. In order to realize the full potential of microreactors for photodegradation, future studies will have to address the problem of designing microreactors that can maximize the efficient incorporation of oxygen.

Acknowledgments

The authors thank Dr. Takayoshi Sasaki for providing the UV lamp used in this work. We are grateful for the assistance provided by Dr. Sakei Nobuyuki and Dr. Tatsuo Shibata in performing spectral measurements. This work was supported by the Special Coordination Funds for Promoting Science and Technology from the Ministry of Education, Culture and Sports, Science and Technology of the Japanese Government.

Literature Cited

- Linsebigler AL, Lu GQ, Yates JT. Photocatalysis on TiO₂ Surfaces—Principles, Mechanisms, and Selected Results. *Chem Rev*. 1995; 95:735–758.
- Konstantinou IK, Albanis TA. TiO₂-assisted photocatalytic degradation of azo dyes in aqueous solution: kinetic and mechanistic investigations—a review. *Appl Catal B—Environ*. 2004;49:1–14.
- Mills A, Wang JS. Photomineralisation of 4-chlorophenol sensitised by TiO₂ thin films. *J Photochem Photobiol A—Chem*. 1998;118:53–63.
- Dijkstra MFJ, Panneman HJ, Winkelman JGM, Kelly JJ, Beenackers A. Modeling the photocatalytic degradation of formic acid in a reactor with immobilized catalyst. *Chem Eng Sci*. 2002;57:4895–4907.
- Ray AK, Beenackers A. Novel photocatalytic reactor for water purification. *AIChE J*. 1998;44:477–483.
- Chen YJ, Dionysiou DD. Effect of calcination temperature on the photocatalytic activity and adhesion of TiO₂ films prepared by the P-25 powder-modified sol-gel method. *J Mol Catal A—Chem*. 2006; 244:73–82.
- Wootton RCR, Fortt R, de Mello AJ. On-chip generation and reaction of unstable intermediates—monolithic nanoreactors for diazonium chemistry: azo dyes. *Lab on a Chip*. 2002;2:5–7.
- Li XY, Wang HZ, Inoue K, Uehara M, Nakamura H, et al. Modified micro-space using self-organized nanoparticles for reduction of methylene blue. *Chem Commun*. 2003;964–965.
- Nakamura H, Li XY, Wang HZ, Uehara M, Miyazaki M, et al. A simple method of self assembled nano-particles deposition on the micro-capillary inner walls and the reactor application for photocatalytic and enzyme reactions. *Chem Eng J*. 2004;101:261–268.
- Gorges R, Meyer S, Kreisel G. Photocatalysis in microreactors. *J Photochem Photobiol A—Chem*. 2004;167:95–99.
- Takei G, Kitamori T, Kim HB. Photocatalytic redox-combined synthesis of L-pipecolic acid with a titania-modified microchannel chip. *Catal Commun*. 2005;6:357–360.
- Jones B, Locascio L, Hayes M. Radical Activated cleavage of peptides and proteins: an alternative to proteolytic digestion. In Jensen KF, Han J, Harrison DJ, Voldman J. *Proceeding of the Micro Total Analysis Systems Conference, 2005, Boston*. San Diego: Transducer Research Foundation; 2005:286–288.
- Hodes G. *Electrochemistry of Nanomaterials*. Weinheim: Wiley-VCH Verlag; 2002.
- Xu NP, Shi ZF, Fan YQ, Dong JH, Shi J, et al. Effects of particle size of TiO₂ on photocatalytic degradation of methylene blue in aqueous suspensions. *Indus Eng Chem Res*. 1999;38:373–379.
- Lakshmi S, Renganathan R, Fujita S. Study on TiO₂-mediated photocatalytic degradation of methylene-blue. *J Photochem Photobiol A—Chem*. 1995;88:163–167.
- Zhang TY, Oyama T, Aoshima A, Hidaka H, Zhao JC, et al. Photo-oxidative N-demethylation of methylene blue in aqueous TiO₂ dispersions under UV irradiation. *J Photochem Photobiol A—Chem*. 2001;140:163–172.
- Mills A, Wang JS. Photobleaching of methylene blue sensitised by TiO₂: an ambiguous system? *J Photochem Photobiol A—Chem*. 1999;127:123–134.
- Lindstrom H, Rensmo H, Sodergren S, Solbrand A, Lindquist SE. Electron transport properties in dye-sensitized nanoporous-nanocrystalline TiO₂ films. *J Phys Chem*. 1996;100:3084–3088.
- Warren B. *X-Ray Diffraction*. New York: Dover Publications; 1969.
- Xu YH, Wang LY, Zhang Q, Zheng SH, Li XJ, et al. Correlation between photoreactivity and photophysics of sulfated TiO₂ photocatalyst. *Mat Chem Phys*. 2005;92:470–474.
- Matthews RW. Photocatalytic oxidation and adsorption of methylene-blue on thin-films of near-ultraviolet-illuminated TiO₂. *J Chem Soc—Faraday Trans I*. 1989;85:1291–1302.
- Ollis DF, Pelizzetti E, Serpone N. Photocatalyzed destruction of water contaminants. *Environ Sci Technol*. 1991;25:1522–1529.
- Solomon TH, Gollub JP. Chaotic particle-transport in time-dependent Rayleigh-Benard convection. *Phys Rev A*. 1988;38:6280–6286.
- Kebede Z, Lindquist SE. The obstructed diffusion of the I-3(-) ion in mesoscopic TiO₂ membranes. *Solar Energy Mat Solar Cells*. 1998;51:291–303.
- Calza P, Pelizzetti E, Minero C. The fate of organic nitrogen in photocatalysis: an overview. *J App Electrochem*. 2005;35:665–673.

Manuscript received July 19, 2006, and revision received Dec. 8, 2006.